International Conference on Space Optics—ICSO 2014

La Caleta, Tenerife, Canary Islands

7–10 October 2014

Edited by Zoran Sodnik, Bruno Cugny, and Nikos Karafolas

Performance characterization of a phase-induced amplitude apodization complex focal plane mask

K. Newman

R. Belikov

O. Guyon

esa icso proceedings cnes

International Conference on Space Optics — ICSO 2014, edited by Zoran Sodnik, Nikos Karafolas, Bruno Cugny, Proc. of SPIE Vol. 10563, 105635K · © 2014 ESA and CNES
CCC code: 0277-786X/17/$18 · doi: 10.1117/12.2304127

PERFORMANCE CHARACTERIZATION OF A PHASE-INDUCED AMPLITUDE APODIZATION COMPLEX FOCAL PLANE MASK

K. Newman[1], R. Belikov[2], O. Guyon[3]

[1]*University of Arizona, College of Optical Sciences, USA. Email: knewman@email.arizona.edu*
[2]*NASA Ames Research Center, Moffett Field, CA, USA.*
[3] *National Astronomical Observatory of Japan (NAOJ), Subaru Telescope, Hilo, HI, USA.*

I. INTRODUCTION

The direct imaging of extrasolar planets is a prominent goal for modern astrophysics. Direct imaging is a technique which can detect some planets that are inherently not compatible with the transit or radial velocity techniques. Direct imaging can also make it possible to measure the spectrum of planet light, which can help to characterize the planet atmosphere. A coronagraph is a telescope instrument with the purpose of enabling direct detection of extrasolar planets and performing exoplanet science. A coronagraph operates by nulling the light from a single on-axis star so that the faint light of a nearby exoplanet can be observed. A typical coronagraph creates a focus of the starlight in the focal plane, and has an element known as a focal plane mask to block or manipulate the starlight. Another element in the pupil plane, known as the Lyot mask, is used to control diffraction from the blocked starlight.

Many coronagraph designs have been developed, and in this paper we focus on a particularly high performance design: the Phase-Induced Amplitude Apodization Complex Mask Coronagraph (PIAACMC) [1,2]. A schematic of the PIAACMC design is shown in Fig. 1. The PIAACMC is a modification of the original PIAA technique [3], which uses aspheric optics to apodize the input pupil. The PIAACMC design uses a partially transmissive focal plane mask to provide a phase shift to a portion of the starlight. A Lyot mask forces the phase-shifted starlight to interfere with the un-shifted starlight in a destructive manner that effectively nulls the star. The design allows for high system throughput, and enables the detection of planets at a small angular separation relative to their host star. One important system characteristic is that it can be designed for almost any pupil geometry [2], including central obscurations, support beams, and segmented apertures; features that are common in large next-generation telescopes.

A remaining challenge is to develop and characterize the focal plane mask for PIAACMC. In section two we describe a design procedure for the focal plane mask and discuss some considerations for advanced mask designs. In section three we simulate the mask performance for given manufacturing errors, and describe a technique for measuring the performance of the mask. In section four we conclude with a broader discussion of mask development.

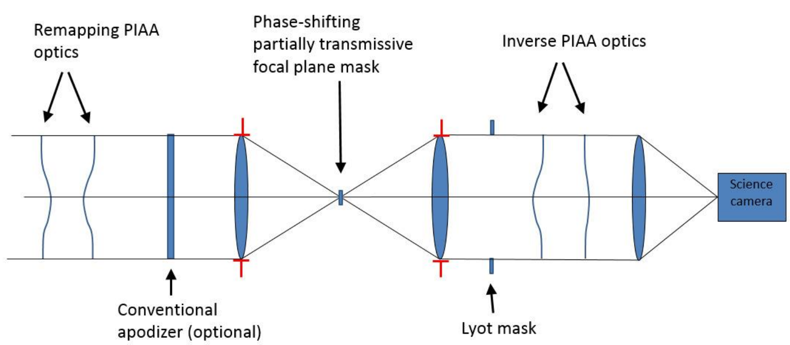

Fig. 1. Schematic of a typical PIAACMC configuration

II. DESIGN

For a given telescope pupil geometry, a PIAACMC system can be designed in three phases. The first two phases are described in greater detail in [2] and we summarize the steps here to provide context. The first phase is to compute the generalized prolate function for apodization. Computing the prolate function assumes a certain focal plane mask size and post-apodizer transmission if necessary. In the second phase, we repeat the computations of the first phase for different focal plane mask sizes and compute the off-axis throughput for a potential exoplanet detection. At the end of the second phase we choose the focal plane mask size to maximize throughput. In this paper we will focus on the third phase of the design, which is to achromatize the focal plane mask.

To create perfect destructive interference, the focal plane mask should provide a pi phase shift to half of the starlight and leave the other half un-shifted. Up to this point in the design process, we have assumed that the focal plane mask operates in monochromatic light. The design of a monochromatic mask is quite simple: for a given mask material and stellar point spread function, the monochromatic mask should be a half wave phase plate that is sized to affect half of the intensity within the PSF. The design can theoretically achieve total on-axis light extinction for a single wavelength. However, coronagraphs can more efficiently produce scientific results by operating in a broad range of wavelengths, typically on the order of 10% or 20% bandwidth. Designing the focal plane mask for a large bandwidth can be challenging, as the mask needs to provide a phase shift achromatically. The mask must overcome the inherent chromaticity of any potential phase plate material, and compensate for the changing size of the stellar PSF with wavelength. So far, there is no analytical solution to achromatize the mask, and we rely on optimization methods to provide a solution that is close to ideal.

After phase two of the PIAACMC system design process, we have a fixed mask size that needs to provide a pi phase shift over a given range of wavelengths. We divide the mask, which at this point is a circularly symmetric disk, into zones. Because the PSF is circularly symmetric, our first approach is to create circular ring zones as shown on the left side of Fig. 2. We have also tried dividing each ring into arc-like segments, and any other geometry for dividing the mask is theoretically possible. We use the Fourier Transform method to compute the diffraction pattern in the pupil plane of each individual zone. The material of the mask is chosen, and the only remaining free parameter is the depth of each zone. We then vary the depth of each zone and compute the combined diffraction pattern. The depth of each zone is optimized to produce the best contrast in the focal plane. An example of a mask, along with the resulting contrast curve is shown in Fig 2. for a 2.4m telescope with a central obscuration and four support beams.

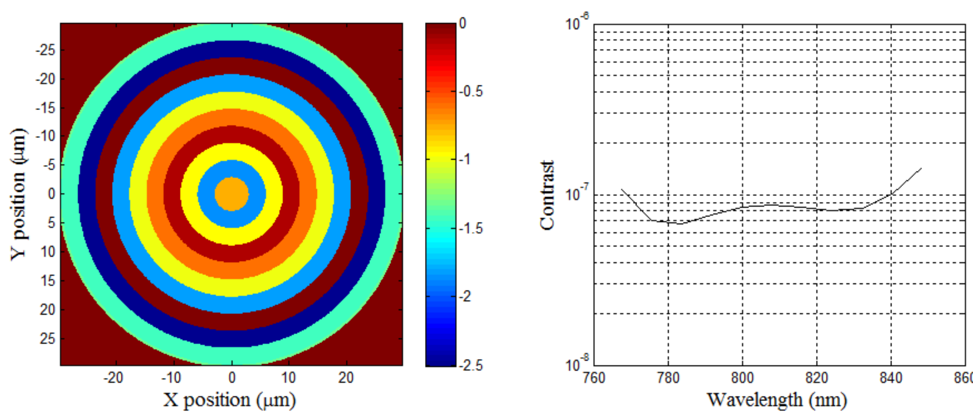

Fig. 2. Depth profile in microns of a PIAACMC mask (left). Contrast of the mask in a region spanning 2-4 λ/D for a 10% range of wavelength (right).

III. CHARACTERIZATION

A. Profile measurement

The optimized depth profile for most masks includes features that are less than a micron in size. Manufacturing the masks is challenging, but not impossible, and pushes the limits of recent advances in nanofabrication. Performance of the mask is particularly sensitive to the accuracy of the zone depths. In simulations, we added errors to the zone ring depths of the mask pattern shown in section II, and calculated the resulting contrast with all other system parameters ideal. The results are shown in Table 1. We did not include any compensation from wavefront control or other methods. Errors were produced randomly from a uniform distribution ranging from zero up to the maximum error, and each error had an even chance to be assigned as positive or negative. The simulation was repeated one hundred times for each value of maximum error, and we report the mean and median contrast between 2-4λ/D for the combination of all simulations. To remain within a factor of 10 or 100 relative to the ideal contrast, errors in the ring depths should remain below an average of 10nm and 40nm respectively. Results may differ for other mask designs, but we can use this as a baseline for discussion of the accuracy needed for manufacturing.

Table 1. Simulated contrast for given manufacturing error in mask ring depth

Maximum error	Mean contrast	Median contrast	Reduction in contrast
0	8.96e-8	8.41e-8	None
10nm	9.05e-7	7.58e-7	10
20nm	3.59e-6	2.71e-6	40
30nm	6.95e-6	5.61e-6	78
40nm	1.38e-5	1.14e-5	154
50nm	1.89e-5	1.48e-5	211
60nm	2.16e-5	2.16e-5	241

Masks similar to the ring design described in section II have been fabricated at the NASA Jet Propulsion Lab Microdevices Lab (MDL) and the Stanford Nanofabrication Facility (SNF). Images of masks fabricated by both facilities are shown in Fig. 3. MDL etched the mask pattern onto a fused silica substrate using electron beam lithography and a Polymethylglutarimide (PMGI) resist, building on experience from fabricating previous mask designs [4]. Interferometry measurements of the depth profile indicate an average error of 65nm and a median error of 48nm from the target depth for all rings. MDL expects to achieve better accuracy with more iterations of mask fabrication. SNF etched a similar mask pattern onto a silicon substrate using electron beam lithography and a proprietary resist. The depth errors for the mask fabricated by SNF are unknown at this time.

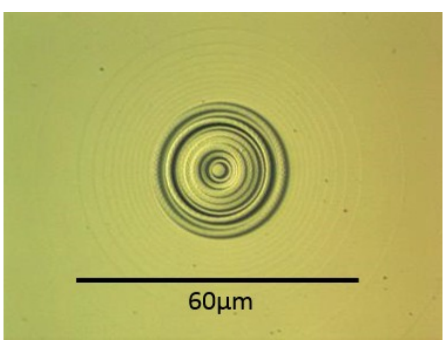

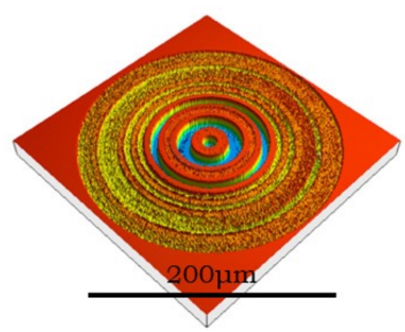

Fig. 3. Microscope image of a mask fabricated at the NASA Jet Propulsion Lab Microdevices Lab (left). White light interferometry measurement of a mask fabricated at the Stanford Nanofabrication Facility (right).

B. Diffraction measurement

The ultimate measure of mask performance is to determine the phase profile produced by the mask. Direct measurement of the profile of the mask using microscopy or interferometry can provide a detailed estimate of the phase profile because mask features are directly related to the phase shift of the mask. However, there are other factors that contribute to mask performance, such as alignment errors of the mask wafer, illumination of the mask, and edge effects from small features of the mask profile. We would prefer to have a method to measure the combined effects of all the system variables: a direct measurement of the phase profile after the mask.

One way to achieve this is to measure the diffraction pattern after the mask using the optical setup shown in Fig 4. In this setup we produce a collimated beam which is stopped down by an iris. The collimated beam is focused onto a reflective focal plane mask, and the reflected beam is directed towards a CCD camera. In one scenario, we move the CCD and take images of the diffraction pattern at various locations along the path of the reflected beam. We can then use a method similar to Gerchberg-Saxton [5] to compute the phase profile just after the mask. An example diffraction pattern, measured after the mask discussed in section II, is shown in Fig. 5. In another scenario, we place the CCD at a plane that is conjugate to the iris. We can then vary the size of the iris and measure the resulting diffraction pattern at the CCD, and use a modified version of the Gerchberg-Saxton algorithm to compute the phase profile of the mask.

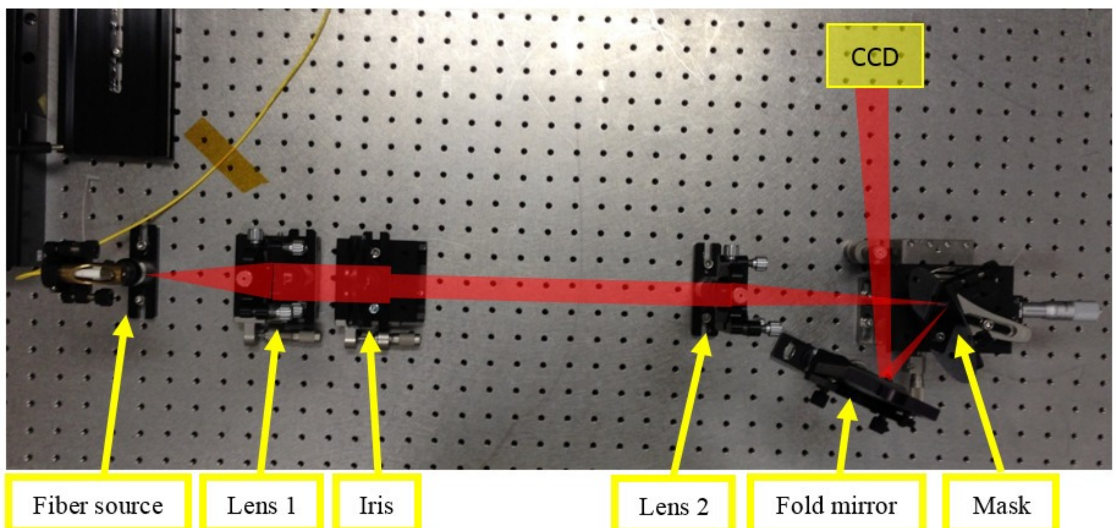

Fig. 4. Image of the optical test layout at the NASA Ames Coronagraph Experiment Lab for measuring the diffraction pattern of a reflective PIAACMC mask.

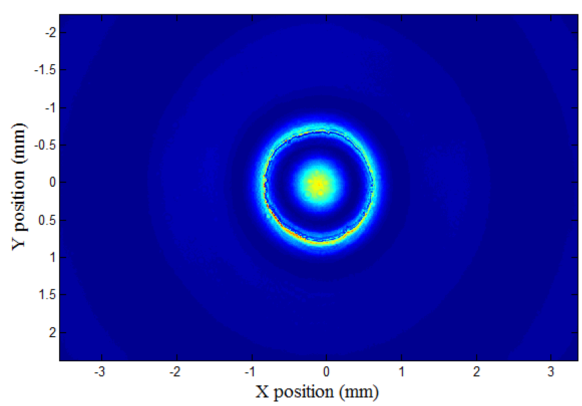

Fig. 5. Diffraction pattern after the focal plane mask.

IV. DISCUSSION AND CONCLUSION

PIAACMC is a high performance coronagraph architecture that is compatible with current and future complex telescope pupils. Successful development of the coronagraph is dependent on characterization of the focal plane mask, which can be a challenging structure to fabricate and measure. We have established methods to optimize the mask profile for high coronagraph performance, but we should also consider manufacturing aspects into the design. For example, it may be easier to manufacture a smooth and continuous profile rather than a series of concentric rings with different depths. Designing for a smooth profile may change the optimization algorithm, but it should be considered to ease manufacturing.

Initial manufacturing results from two separate institutions have shown that the mask profiles are challenging, but not impossible to fabricate. Simulations show that coronagraph performance is highly dependent on accuracy of the mask profile, and manufacturing methods have not yet consistently achieved the accuracy needed for optimal performance. The use of compensators, such as wavefront control, could alleviate the tolerances needed for mask manufacturing. We expect the accuracy of manufacturing to improve with more experience.

We have begun developing a method to directly measure the phase profile after the focal plane mask, based on diffraction measurements and a Gerchberg-Saxton type of algorithm. We expect to have computational results from this method in the coming months. Measurement of the phase profile will be used as a performance metric for the mask, and will provide feedback that can be used in the mask design process.

REFERENCES

[1] O. Guyon, F. Martinache, R. Belikov, R. Soummer, "High performance PIAA coronagraphy with complex amplitude focal plane masks," ApJ 190, 2010.
[2] O. Guyon, P. Hinz, E. Cady, R. Belikov, F. Martinache, "High performance lyot and PIAA coronagraphy for arbitrarily shaped telescope apertures," ApJ 780, 2013.
[3] O. Guyon, "Phase-Induced Amplitude Apodization of Telescope Pupils for Extrasolar Terrestrial Planet Imaging", A&A v.404, p. 379-387, 2003.
[4] K. Balasubramanian, et al., "High contrast internal and external coronagraph masks produced by various techniques," Proc. SPIE, Vol. 8864, 2013.
[5] R. Gerchberg, W. Saxton, "A Practical Algorithm for the Determination of Phase from Image and Diffraction Plane Pictures," Optik Vol. 35, 237-246, 1972.